Cholesterol in Bilayers with PUFA Chains: Doping with DMPC or POPC Results in Sterol Reorientation and Membrane-Domain Formation[†]

Norbert Kučerka,*,‡,§ Drew Marquardt,‖ Thad A. Harroun,‖ Mu-Ping Nieh,‡ Stephen R. Wassall,⊥ Djurre H. de Jong,# Lars V. Schäfer,# Siewert J. Marrink,# and John Katsaras*,‡,△

‡Canadian Neutron Beam Centre, National Research Council, Chalk River, Ontario K0J 1J0, Canada, §Department of Physical Chemistry of Drugs, Comenius University, 835 35 Bratislava, Slovakia, ‖Department of Physics, Brock University, St. Catherines, Ontario L2S 3A1, Canada, ⊥Department of Physics, Indiana University–Purdue University Indianapolis, Indianapolis, Indiana 46202, #Groningen Biomolecular Sciences and Biotechnology Institute and Zernike Institute for Advanced Materials, University of Groningen, Groningen, The Netherlands, and △Guelph-Waterloo Physics Institute and Biophysics Interdepartmental Group and Department of Physics, University of Guelph, Guelph, Ontario N1G 2W1, Canada

ABSTRACT: Using neutron diffraction Harroun et al. [(2006) *Biochemistry 45*, 1227–1233; (2008) *Biochemistry 47*, 7090–7096] carried out studies that unequivocally demonstrated cholesterol preferentially sequestering in the middle of bilayers (i.e., flat orientation) made of lipids with polyunsaturated fatty acids (PUFA), in contrast to its "usual" position where its hydroxyl group locates near the lipid/water interface (i.e., upright orientation). Here we clearly show, using neutron diffraction, cholesterol's orientational preference in different lipid bilayers. For example, although it requires 50 mol % POPC (16:0−18:1 PC) in DAPC (di20:4 PC) bilayers to cause cholesterol to revert to its upright orientation, only 5 mol % DMPC (di14:0 PC) is needed to achieve the same effect. This result demonstrates not only cholesterol's affinity for saturated hydrocarbon chains, but also its aversion for PUFAs. Molecular dynamics (MD) simulations performed on similar systems show that in high PUFA content bilayers cholesterol is simultaneously capable of assuming different orientations within a bilayer. Although this result is known from previous MD studies by Marrink et al. [(2008) *J. Am. Chem. Soc. 130*, 10−11], it has yet to be confirmed experimentally. Importantly, MD simulations predict the formation of DMPC-rich domains, data corroborated by experiment (i.e., 10 mol % DMPC-doped DAPC bilayers), where cholesterol preferentially locates in its upright orientation, while in DMPC-depleted domains cholesterol is found mostly in the bilayer center (i.e., flat orientation). These results lend credence to DMPC's aversion for PUFAs, supporting the notion that domain formation is primarily driven by lipids.

One of the main building blocks of cellular membranes is lipids, a diverse family of molecules which form two-dimensional (2D) fluid matrices and in which membrane-associated proteins are able to carry out their various functions. In 1972, Singer and Nicolson (*1*) proposed the "fluid mosaic" model to describe the structural features of biological membranes. Although the basic premise of this model (i.e., integral proteins diffusing more or less freely in a 2D viscous phospholipid bilayer solvent) still applies, the plasma membrane has since been shown to be considerably more complex, especially with regard to the diversity and function of its lipid components (*2*). An example of this is lipid rafts, regions of membranes enriched in certain types of lipids (predominantly saturated sphingolipids) and cholesterol, and which are thought, in biological membranes, to act as functionalized platforms (*3*).

Much of our current understanding regarding rafts comes from studies of lateral phase separation in model membranes composed of ternary mixtures of saturated and unsaturated lipids, including cholesterol. Formation of these domains is assumed to be the result of distinct interactions between cholesterol and lipids with different hydrocarbon chains, causing cholesterol to partition preferentially with saturated hydrocarbon chain lipids, forming a liquid ordered phase (*4−6*).

Cholesterol is found in all animal cell membranes and is required for proper membrane permeability and fluidity. It is also needed in the building and maintenance of cell membranes and is thought to act as an antioxidant (*7*). As mentioned, cholesterol has also been implicated in cell signaling processes, where it has been suggested that it enables the formation of rafts in the plasma membrane (*8*, *9*). The recent controversies regarding the physiological implications of so-called "good" (high-density lipoprotein or HDL) and "bad" (low-density lipoprotein or LDL) cholesterol have also brought to prominence the importance of cholesterol's biosynthetic pathways and transport to and from cells.

Among the other sterols, cholesterol has been shown to be the most effective in inducing membrane ordering in binary lipid/sterol mixtures (*10*), where cholesterol tilt angle has been implicated as being an important parameter (*11*). It has also been shown that cholesterol dramatically "stiffens" bilayers composed of

*Corresponding authors. N.K.: e-mail, Norbert.Kucerka@nrc.gc.ca; phone, (613) 584-8811; fax, (613) 584-4040. J.K.: e-mail, John.Katsaras@nrc.gc.ca; phone, (613) 584-8811; fax, (613) 584-4040.

saturated lipids, while it interacts much more weakly with unsaturated chain lipids (*12*). Nevertheless, even in the case of dimonounsaturated lipids the observed thickness increase in bilayers containing cholesterol suggests that the hydrocarbon ordering effect induced by cholesterol still dominates over its ability to reduce the hydrophobic mismatch between itself and the lipid fatty acid chains (*13*, *14*). This situation, however, is in stark contrast when compared to lipids containing polyunsaturated fatty acids (PUFA)[1] (*15*). For example, in the case of lipids with PUFA hydrocarbon chains there seems to be a strong aversion of the highly disordered PUFAs to cholesterol's planar rigid surface, an interaction thought to be the major driving force in domain formation. In biological membranes, such lateral sequestration of PUFA lipids into membrane domains depleted of cholesterol has been hypothesized to have an important role in neurological function and in alleviating a number of health-related issues (*16*).

PUFAs constitute a biologically influential group of molecules. Both omega-3 and omega-6 classes of PUFAs are essential for normal growth and development, and are only available through diet as they cannot be synthesized from other components by any known biochemical pathway (*17*). Importantly, the dietary consumption of PUFAs, in particular omega-3 fatty acids, is known to alleviate a number of chronic health conditions (*18*). For example, they have been suggested to play an important role in the prevention and treatment of coronary artery disease, hypertension, diabetes, arthritis, other inflammatory and auto-immune disorders, and cancer. On the other hand, a diet rich in omega-6 fatty acids was linked to a shift in physiologic state to one that is prothrombotic and proaggregatory, with increases in blood viscosity, vasospasm, and vasoconstriction (*19*). While the general consensus considers omega-3 PUFAs to be partial agonists relative to those of the omega-6 class, their induced structural effects on the properties of biological membranes are presently not clear for either of these groups.

Recently, neutron studies of DAPC (diC20:4PC) bilayers, lipids containing omega-6 PUFAs, found cholesterol sequestered inside the membrane with the steroid moiety and side chain lying in the middle of and parallel to the plane of the membrane (flat orientation) (*20*, *21*). This situation is in contrast to its "usual" position where cholesterol's hydroxyl group locates near the lipid/water interface and where the sterol molecule, which lines up with the acyl chains parallel to the bilayer normal, extends toward the membrane's center. Molecular dynamics (MD) simulations using the MARTINI coarse-grained force field have also shown that cholesterol's tilt angle with respect to the bilayer normal varies with the number of double bonds present in the lipid fatty acid chains (*22*), i.e., positive correlation between increasing hydrocarbon chain unsaturation and increasing cholesterol tilt angle. It was also shown that cholesterol flip-flop frequency between bilayer leaflets dramatically increases with the number of double bonds. It is therefore enticing to think that cholesterol's increased flip-flop rate in the presence of PUFA lipids may be associated with a cell-signaling response mechanism to changes in membrane fluidity or stress. Consequently, it may well be that in a mixed bilayer of saturated and polyunsaturated lipids cholesterol is able to reorient between its upright and flat orientations.

We have carried out neutron diffraction experiments to test whether or not cholesterol can revert to its upright position at some critical concentration of monounsaturated (POPC) or fully saturated (DMPC) lipid in PUFA bilayers. Over the years the interaction of cholesterol with saturated fatty acids has been well characterized. It is known that the introduction of the rigid steroid moiety into saturated lipid membranes disrupts the regular packing of the fatty acid chains in the gel, or solid ordered (so) phase, and restricts the reorientation of the fatty acid chains in the liquid crystalline, or liquid disordered (ld) phase (*23*). The differential between the two phases is smeared out by the liquid ordered (lo) phase, which is characterized by the rapid reorientation but high conformational order of the fatty acid chains and which is formed over a wide range of temperatures and concentrations exceeding approximately 16 mol % cholesterol. As mentioned, within most common membranes cholesterol orients in its upright orientation (*24*). Its individual molecules rotate rapidly about their long axis, while undergoing a wobble through a narrow range of angles, slightly tilted relative to the bilayer normal (*25*). In contrast to its affinity for saturated lipid bilayers, cholesterol's relationship with disordered unsaturated bilayers is complicated to the point that in mixed systems phase separation may occur (*16*). It should be pointed out that cholesterol may regulate membrane fluidity not just by the formation of lateral domains, as is so much the focus of lipid raft research, but also by its wholesale movement across the bilayer, which in turn controls membrane protein function (*9*). Although it is known that cholesterol's presence in phospholipid bilayers decreases both their fluidity and permeability (*26*), this becomes an open question when cholesterol sequesters itself in the bilayer center.

Neutron diffraction experiments determined the orientation of cholesterol as a function of lipid species and concentration. In agreement with previous results, cholesterol is found lying parallel in the bilayer center (*15*, *20–22*) at low concentrations of POPC in DAPC bilayers. However, at a certain critical lipid concentration of POPC (~50 mol %), cholesterol reorients to its upright position. Interestingly, the amount of DMPC necessary to flip cholesterol in DAPC bilayers is only a small fraction (~5 mol %) of that of POPC, clearly demonstrating cholesterol's preference for saturated fatty acid chain lipids. Importantly, our experimental results for >5 mol % DMPC, also supported by MD simulations data, suggest the formation of lateral domains within DAPC bilayers. In light of the present data, we thus propose a simple interaction model of lipid fatty acid chains with cholesterol.

MATERIALS AND METHODS

Neutron Diffraction. Polyunsaturated bilayers of 1,2-diarachidonoylphosphatidylcholine (diC20:4PC, DAPC) were doped either with monounsaturated 1-palmitoyl-2-oleoylphosphatidylcholine (C16:0–18:1PC, POPC) or the saturated lipid 1,2-dimyristoylphosphatidylcholine (diC14:0PC, DMPC). All lipids were obtained from Avanti Polar Lipids (Alabaster, AL). Unlabeled cholesterol was ordered from Sigma-Aldrich (St. Louis, MO), while the headgroup deuterated (2,2,3,4,4,6-d_6) cholesterol was purchased from C/D/N Isotopes (Pointe-Claire, QB). Upon arrival the ampules containing the various lipids were stored at −80 °C and samples were randomly checked for degradation using thin-layer chromatography. All samples were prepared using reagent grade solvents.

Approximately 12 mg of lipid containing appropriate amounts of DAPC and DMPC, or DAPC and POPC, was codissolved in a

---

[1] Abbreviations: PUFA, polyunsaturated fatty acids; MD, molecular dynamics; CG, coarse-grained; DAPC, 1,2-diarachidonoylphosphatidylcholine (diC20:4PC); POPC, 1-palmitoyl-2-oleoylphosphatidylcholine (C16:0-18:1PC); DMPC, 1,2-dimyristoylphosphatidylcholine (diC14:0PC); NSLD, neutron scattering length density.

mixture of chloroform and trifluoroethanol and mixed with 10 mol % of labeled or unlabeled cholesterol; care was taken to prevent exposure of the lipids to oxygen. Each sample was then deposited onto the surface (25×60 mm^2) of a 1 mm thick silicon wafer and rocked during evaporation of the organic solvent in a glovebox filled with nitrogen. The samples were then dried in a vacuum for several hours (usually overnight).

Neutron diffraction data were collected at the Canadian Neutron Beam Centre's D3 beamline located at the National Research Universal (NRU) reactor (Chalk River, Ontario, Canada) using 2.37 Å wavelength neutrons. The appropriate wavelength neutrons were selected by the (002) reflection of a pyrolytic graphite (PG) monochromator, while a PG filter was used to eliminate higher order reflections (i.e., $\lambda/2$, $\lambda/3$, etc.). Samples were placed in an airtight sample cell (27) and hydrated to the requisite relative humidity (RH) using a series of D$_2$O/H$_2$O mixtures (i.e., 100%, 70%, and 8% D$_2$O). RH was controlled by saturating the various D$_2$O/H$_2$O solutions with KCl (84% RH). Experimental stability over the course of data collection was confirmed by the reproducibility of the diffraction data, whereby it was sought that lamellar repeat spacings and peak intensities remained constant over time, thus indicating that the sample
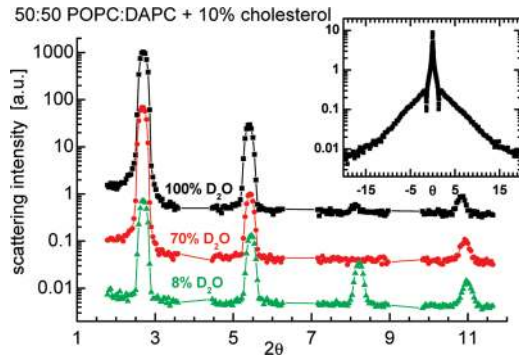

FIGURE 1: An example of raw neutron diffraction data. The main graph plots scattering intensity as a function of the scattering angle, 2θ. Diffraction data from a 50:50 POPC:DAPC + 10 mol % cholesterol sample hydrated from water vapor with different percent D$_2$O (i.e., 100%, 70%, and 8%) are shown. The data are shifted vertically for better viewing. The inset to the graph shows a typical rocking curve (i.e., where the sample position, θ, is fixed and the detector angle, 2θ, is scanned) that was used to assess sample quality.

chemistry and sample conditions remained unaltered. It was found that some samples deteriorated after several hours, most likely the result of the high susceptibility of PUFA hydrocarbon chains to peroxidation. These samples were excluded from the analysis.

The quality of sample alignment was assessed from rocking curves (i.e., the sample was rotated at a fixed detector angle). Most samples displayed a sharp peak (see inset to Figure 1) corresponding to large lateral domains of highly oriented multibilayers. This sharp peak usually sits atop of a broad peak consisting of scattering from much smaller domains with a broader distribution of orientations (28). In the case of some samples the lack of a central sharp peak suggests a specimen with numerous small domains with slightly different orientations from each other.

Typically up to four orders of Bragg diffraction were obtained. Changes in contrast resulted in changes to the scattered intensities, but not to peak positions (Figure 1). The diffraction peaks obtained from $\theta-2\theta$ scans, where θ and 2θ are the angles of the sample and the detector, respectively, were fitted to Gaussians with an additional second-order polynomial function used to describe the background. Integrated intensities for the different quasi-Bragg peaks were corrected for incident flux (C_{flux}), sample absorption (C_{abs}), and the Lorentz correction (C_{Lor}) according to well-established procedures (29). The uncertainties associated with the obtained scattering form factors were estimated from repeated diffraction scans while assuming a 95% confidence interval. The corrected form factors F_h (Table 1) were then used to determine the phases, which were subsequently Fourier transformed into neutron scattering length density (NSLD) profiles using

$$\Delta\rho^{exp}(z) = \frac{2}{D}\sum_{h=1} F_h^{exp} \cos\left(\frac{2\pi hz}{D}\right) \qquad (1)$$

where $\Delta\rho$ stands for the water subtracted profile (i.e., $\Delta\rho(z) = \rho(z) - \rho_w$) and D is the sample's lamellar repeat spacing.

Finally, the data were placed on an absolute scale using

$$\Delta\rho^{abs}(z) = c + k\Delta\rho^{exp}(z) \qquad (2)$$

by requiring that NSLD profiles possess the correct values at given points along the bilayer (e.g., bilayer/water interface and bilayer center) and that the area from the difference NSLD

Table 1: Corrected Experimental Form Factors in Units of 1e^{-6} Å^{-1}

	protonated cholesterol			deuterated cholesterol		
	8% D$_2$O	70% D$_2$O	100% D$_2$O	8% D$_2$O	70% D$_2$O	100% D$_2$O
POPC, 30%						
F_1	-18.0 ± 0.2	-43.5 ± 0.5	-63.2 ± 0.5	-15.3 ± 0.8	-42.0 ± 0.6	-62.4 ± 0.8
F_2	-5.43 ± 0.07	5.38 ± 0.28	11.2 ± 0.6	-6.17 ± 0.26	8.06 ± 0.40	14.9 ± 0.7
F_3	4.14 ± 0.03	1.04 ± 0.95	0	5.17 ± 0.25	1.52 ± 0.08	0
F_4	-2.09 ± 0.02	-1.48 ± 0.23	-1.38 ± 0.07	-2.73 ± 0.14	-2.23 ± 0.12	-2.06 ± 0.10
POPC, 50%						
F_1	-21.2 ± 0.5	-64.3 ± 1.7	-76.2 ± 1.9	-21.6 ± 0.6	-63.9 ± 3.1	-75.9 ± 0.9
F_2	-8.77 ± 0.23	7.20 ± 0.18	12.8 ± 0.3	-10.2 ± 0.3	6.04 ± 0.31	11.9 ± 0.1
F_3	4.32 ± 0.07	0.33 ± 0.01	-0.99 ± 0.03	5.01 ± 0.09	0.67 ± 0.02	-0.76 ± 0.02
F_4	-2.55 ± 0.18	-2.20 ± 0.06	-1.88 ± 0.08	-2.52 ± 0.06	-1.97 ± 0.07	-1.74 ± 0.05
DMPC, 5%						
F_1	-10.4 ± 0.6	-54.1 ± 0.8	-69.0 ± 2.1	-12.1 ± 0.1	-52.6 ± 2.1	-70.0 ± 1.7
F_2	-7.52 ± 0.37	5.21 ± 0.13	11.7 ± 0.3	-8.51 ± 0.03	3.60 ± 0.15	9.10 ± 0.09
F_3	2.50 ± 0.12	0.56 ± 0.03	-2.16 ± 0.07	3.03 ± 0.04	0	-1.09 ± 0.03
F_4	-1.29 ± 0.06	-1.24 ± 0.06	-1.40 ± 0.05	-1.00 ± 0.08	-0.62 ± 0.02	-0.66 ± 0.02

The uncertainties were estimated from repeated diffraction scans while assuming a 95% confidence interval.

profile corresponded, within experimental error, to the neutron scattering length difference between six deuterium and six hydrogen atoms (*30*).

Molecular Dynamics Simulations. All simulations were carried out using the MARTINI coarse-grained (CG) force field (*31*) implemented within the Gromacs 4.0.5 package (*32*) and applying a 20 fs integration time step along with standard settings for the nonbonded interactions (*31*). Constant particle number, pressure, and temperature (NpT) ensembles were simulated while utilizing periodic boundary conditions. The system was coupled to a pressure bath (1 bar, $\tau_p = 0.3$ ps) using the semi-isotropic coupling scheme. Different molecule types were coupled separately to a heat bath at 300 K using stochastic temperature coupling (inverse friction constant $\tau_T = 5$ ps).

Lipid bilayers with a randomly mixed lateral lipid distribution were used as initial structures and comprised of a total of 1368 PC lipids, 152 cholesterol molecules, and 12600 CG water beads (note that one CG water bead represents four water molecules). The ratio of DMPC, POPC, and PUFA lipids (DAPC) was varied in accordance with the experimentally studied systems and were energy-minimized (100 steps of steepest descent) prior to simulations. The individual simulation times were 2.9, 1.3, and 1.4 μs for systems with 10, 30, and 50 mol % POPC, respectively, and 3.2 and 2.9 μs for systems with 5 and 10 mol % DMPC, respectively. The last 1 μs for simulations with 5 and 10 mol % dopant molecules was analyzed; for the systems with 30 and 50 mol % dopant molecules, analyzing the last 700 ns was found to be sufficient. No net changes to the lateral lipid distribution were observed after the discarded equilibration time, i.e., domain formation was completed. The number distributions and profiles of neutron scattering length densities were calculated according to a procedure described previously (*22*).

RESULTS AND DISCUSSION

Neutron Diffraction. A series of POPC-doped and DMPC-doped DAPC bilayers containing 10 mol % cholesterol were measured using small angle neutron diffraction. The phases of the measured form factors were determined by linear interpolation as a function of D_2O/H_2O contrast (*29*), while the NSLD profiles were reconstructed from the data using eq 1. The amount and resolution of the experimental data were increased through the use of specific labeling, with the end result being the accurate determination of the label's position along the bilayer (*33*). Difference NSLD profiles from lipid bilayers containing labeled and unlabeled cholesterol (see Materials and Methods) were used to accurately determine, in effect, the position of the cholesterol's hydroxyl group.

Samples hydrated with 100% D_2O are best suited for the determination of the bilayer's overall structure (i.e., total thickness, area per lipid, etc.) because of the excellent contrast provided between the hydrating medium and the bilayer (*34*). On the other hand, small structural details are more obvious in samples with NSLDs of small amplitudes making certain structural details easier to observe. For example, fine structural detail is best observed in lipid bilayers hydrated with 8 mol % D_2O rather than 100 mol % D_2O, where the D_2O signal dominates the NSLD profile. In the 8 mol % D_2O case the water contribution has a net zero NSLD; thus the bilayer structure is not obscured by scattering from the solvent. Nevertheless, all of the difference profiles obtained from samples hydrated with various percent D_2O solutions should result in the same distribution function. This is due to the fact that both the NSLD associated with the
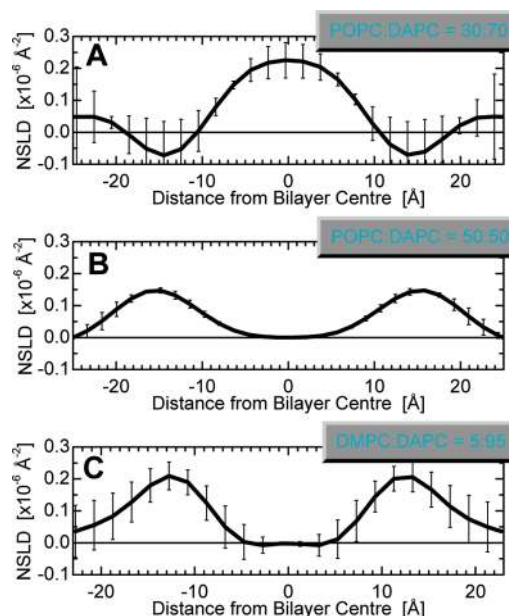

FIGURE 2: NSLD difference profiles showing the distribution of cholesterol's deuterium label (effectively its hydroxyl group) in (A) 30 mol % and (B) 50 mol % POPC-doped DAPC bilayers, and (C) 5 mol % DMPC-doped DAPC bilayers.

lipid and that of the hydrating medium are subtracted with the end result corresponding to the difference between the labeled and unlabeled sample NSLDs (i.e., six deuterium minus six hydrogen atoms per cholesterol molecule) (*30*). To increase the statistics of the experimental measurements, we present results as averages from all of the difference profiles (i.e., 100%, 70%, and 8% D_2O contrast conditions), along with their corresponding error bars. The data shown in Figure 2 are consistent with those previously reported, which only employed data from 8% D_2O samples (*15*).

The results shown in Figure 2 clearly show cholesterol's two very different orientations in DAPC bilayers. Harroun et al. have previously shown that cholesterol is sequestered in the bilayer center of pure DAPC bilayers (*21*). Consistent with the Harroun et al. result, we have observed the same location for cholesterol in DAPC bilayers doped with small amounts of POPC. Figure 2A shows the difference NSLD profile corresponding to DAPC bilayers containing 30 mol % POPC, where the cholesterol label is clearly observed in the bilayer center. We should note that this is the highest POPC concentration in which cholesterol is unambiguously observed in the bilayer center. On the other hand, the above-mentioned situation becomes very different with increasing amounts of POPC.

Figure 2B shows the difference NSLD profile for DAPC bilayers containing 50 mol % POPC, the lowest concentration at which we unambiguously observe cholesterol in its upright orientation. The deuterium label appears to be approximately 15 Å from the bilayer center, placing cholesterol's hydroxyl group within the bilayer's hydrophobic/hydrophilic interfacial region and in agreement with previous data (*14*, *20*). This observation confirms the notion that cholesterol's orientation can be altered by changing the ratio of PUFA/saturated chain lipids. Considering the lipid heterogeneity of biological membranes, this result may be viewed as a prerequisite for the mechanism by which cholesterol transports through the cell membrane.

While previous studies revealed the high propensity of cholesterol to flip-flop between the two leaflets of disordered bilayers
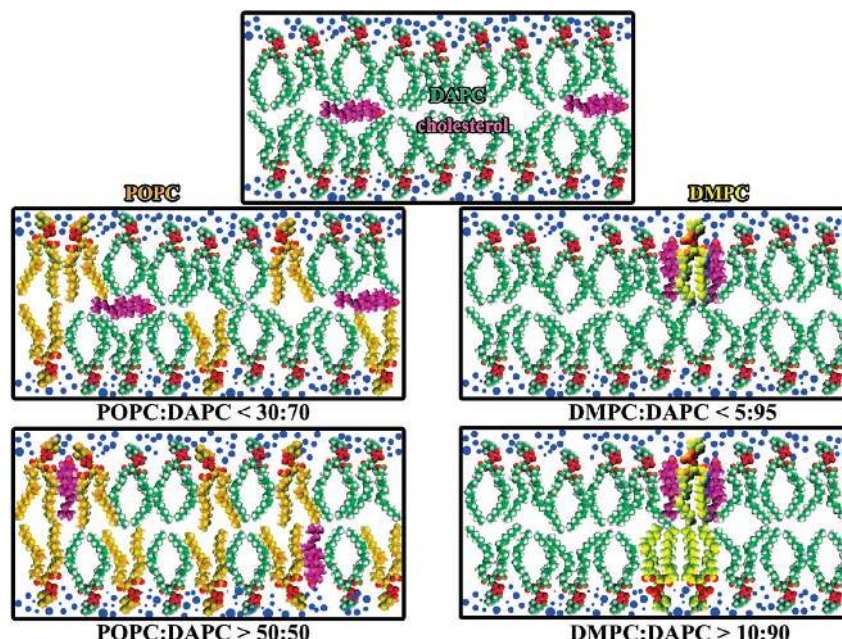
FIGURE 3: Schematics showing the interactions between the different lipids studied and cholesterol. While in the case of POPC the lipid−lipid interaction is favorable, compared to the lipid−cholesterol interaction, it is the strong aversion between saturated and PUFA chains that drives the macromolecular assembly in DMPC-doped DAPC bilayers.

(*14*, *22*), the present results suggest that saturated chain lipids can stabilize such movements. In plasma membranes, for instance, the transbilayer distribution of lipids is typically asymmetric (*35*). PUFA-containing phospholipids are more prevalent in the inner monolayer (*36*), while the outer monolayer is where saturated sphingolpids are mostly found (*37*). By pushing cholesterol to the center of the membrane, a PUFA-rich domain on one side would enhance the transfer of the sterol to a lipid raft on the other. It is even possible to imagine this mechanism resulting in the formation of functionalized domains that could facilitate biosynthetic pathways of cholesterol and its transport to and from cells.

At this point it is worth discussing the concentration (i.e., 50 mol %) of POPC required to flip cholesterol to its upright orientation in DAPC bilayers. Assuming that each POPC is capable of shielding two cholesterol molecules from water, thus reducing the energy penalty (*38*), it follows that the remaining POPC molecules mix with DAPC at a mole ratio of about 1:1. According to our model, the 50 mol % POPC-doped DAPC system provides enough POPCs to shield all of the cholesterol molecules and at the same time associate, on average, with at least one DAPC molecule. However, when the POPC concentration is insufficient to satisfy both of the suggested interactions, cholesterol molecules are expelled into the bilayer center, while the remaining POPC continues to interact with the PUFA chain lipids. In other words, the cross-molecular interaction preference from most to least preferred is (a) POPC−PUFA, (b) POPC−cholesterol, and (c) cholesterol−PUFA (Figure 3).

Compared to POPC-doped DAPC bilayers, the situation is very different in the case of DMPC-doped DAPC bilayers. While 50 mol % POPC is required to flip cholesterol to its upright orientation, Figure 2C shows that only 5 mol % of DMPC is necessary to achieve the same effect. This result clearly demonstrates cholesterol's affinity for saturated chain lipids. Of significance is that the mole ratio of two cholesterols per DMPC corresponds to the maximum solubility of cholesterol in PC bilayers (*38*). It therefore appears that instead of PUFA−DMPC interactions, at this DMPC concentration all DMPCs associate
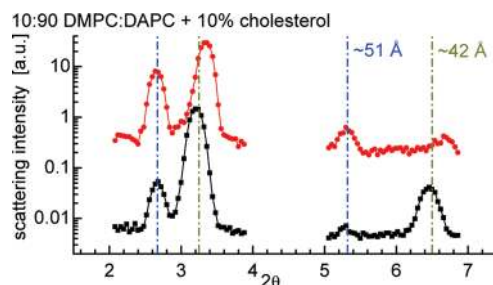

FIGURE 4: Example of raw neutron diffraction data obtained from samples exhibiting two lamellar repeat spacings, which can be associated with DAPC-rich (∼42 Å) and DMPC-rich (∼51 Å) domains. Only the first two diffraction peaks are presented. The data shown were obtained at different times over the course of the experiment and are shifted vertically for better viewing.

with cholesterol molecules. In other words, one DMPC molecule can flip two cholesterol molecules to their upright orientation (see Figure 3).

Up to now all samples studied, especially those that were doped with POPC, resulted in regularly spaced bilayers with well-defined quasi-Bragg peaks (see Figure 1) indicative of equidistant, homogeneous composition bilayers. However, in the case of 10 mol % DMPC-doped DAPC bilayers containing cholesterol, the situation is different. These samples exhibit two lamellar repeat spacings (Figure 4) that correspond to two different composition samples or phase-separated macroscopic domains with extended correlation lengths, a result corroborated by molecular dynamics (MD) simulations of a similar ternary system (*39*). It is important to note that neither of the observed repeat spacings correspond to that of cholesterol monohydrate crystals which exhibit a repeat spacing of ∼34 Å (*38*). It therefore appears that in a system where the DMPC/cholesterol ratio exceeds 1:2, the excess DMPC molecules form DMPC-rich domains to avoid the less preferred PUFA−DMPC interaction (see Figure 3).

The type of neutron diffraction experiments performed in this study provides structural information along the bilayer normal

but does not allow for the direct evidence of lateral domains. It is important to understand that the observation of a single lamellar spacing observed in all POPC-doped samples, and some DMPC-doped samples, does not rule out the existence of domains. For example, the two sets of Bragg peaks can overlay each other if the lamellar spacings are similar, or the two phases may be dispersed homogeneously throughout the sample, resulting in one lamellar repeat spacing. However, the data presented in Figure 4 can only be reconciled by the presence of two different phases, with each phase being in register from one bilayer to the next (i.e., long-range correlation length), something that has been observed previously (*40*).

It is also interesting to note that the lamellar repeat spacing of the 10 mol % DMPC sample ranged, in the case of one phase, from 40 to 45 Å (over the course of one experiment), values close to the 46 Å repeat spacing measured for pure DAPC bilayers with cholesterol (*20*). In the case of the other phase, the lamellar repeat spacing ranged from 48 to 53 Å, consistent with lamellar repeat spacing from pure DMPC (*41, 42*) and DMPC−cholesterol bilayers (*24*). In addition, the ratio of the Bragg peaks associated with these two phases changed as a function of time, suggesting that the domains were also changing over the course of the experiment. It should be pointed out, however, that these samples never formed one pure phase (i.e., one set of Bragg reflections) as observed over a period of 19 h. On the basis of the relative changes of the diffracted intensities, we conclude that the 10 mol % DMPC-doped DAPC system consisted predominantly of a DAPC-like phase early on in the experiment and reached equilibrium with a considerable fraction of the sample containing DMPC-rich domains.

Molecular Dynamics Simulations. Neutron diffraction results were corroborated with MD simulations performed on same composition samples. NSLD profiles obtained from MD simulations are shown in Figure 5. With increasing concentration of the dopant molecule (i.e., POPC or DMPC), there is an increased probability of finding cholesterol's headgroup approximately 14−15 Å from the bilayer center, in the case of POPC, and slightly closer to the bilayer center, in the case of DMPC. The MD results are in qualitative agreement with the neutron diffraction experiments. The difference between experiment and MD simulation is that simulations capture cholesterol in various orientations (i.e., from upright to flat, including flip-flops) (*22*), while up to now, experiments have shown cholesterol (within bilayers) either in its upright or flat orientation, never both simultaneously.

MD simulations predict the formation of DAPC-depleted lateral domains, where cholesterol is oriented upright. In the PUFA-rich domain, most cholesterol molecules adopt the flat orientation, and frequent flip-flops of cholesterol molecules between the bilayer leaflets are observed. In this respect, the MARTINI CG model seems to provide a more realistic description of the cholesterol orientation and flip-flop compared to current atomistic force fields. Specifically, it has been shown that atomistic force fields tend to overestimate the energy barrier for adopting the flat orientation (*43*).

Importantly, both experiment and simulation concur that cholesterol has a much higher affinity for the saturated acyl chain(s) of POPC and DMPC, rather than for the PUFA chains in DAPC, something that is well-known from literature (*4, 43−45*). For example, low solubility (*46*) and reduced partition coefficients (*47*) have been reported for the sterol with PUFA-containing phospholipids. Cholesterol's affinity for saturated lipids or,
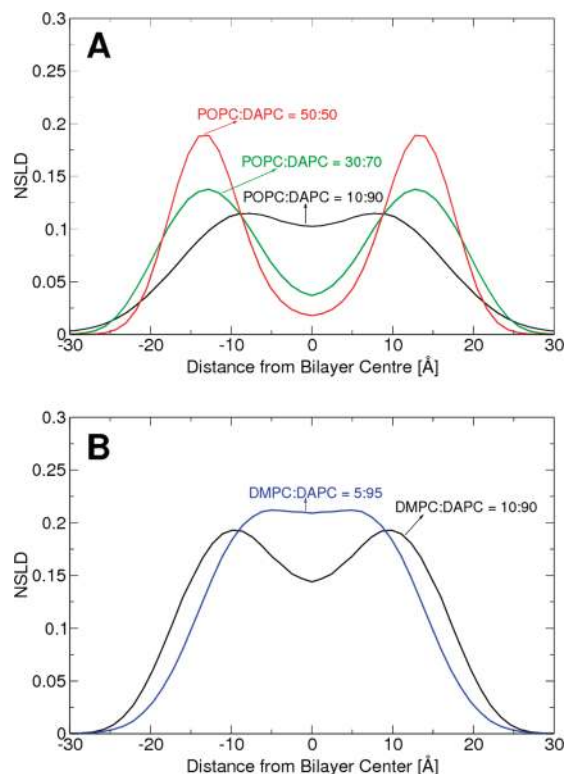

FIGURE 5: NSLD profiles showing the distributions of cholesterol's hydroxyl group as determined by MD simulations. (A) DAPC bilayers doped with 50 mol % POPC (red), 30 mol % POPC (green), and 10 mol % POPC (black). (B) DAPC bilayers doped with 5 mol % DMPC (blue) and 10 mol % DMPC (black). Profiles were calculated as described in ref *22.*

more precisely, the large difference in cholesterol affinities between PUFAs and saturated fatty acids is assumed to be the driving force for the formation of cholesterol-rich domains (*47*). An example of this is the model membrane system made up of cholesterol, DPPC (diC16:0PC), the PUFA chain lipid diC22:6PC, and rhodopsin (*48*). For this particular system there is a large difference in cholesterol's partition coefficient between diC22:6PC and DPPC bilayers, which manifests itself in the formation of DPPC−cholesterol-rich and diC22:6PC−rhodopsin−cholesterol-depleted domains. However, looking at it from a different point of view, one can argue that rather than cholesterol's differing affinities for the two lipids (i.e., diC22:6PC and DPPC), domain formation may be the result of the aversion that the two lipid species may have for each other, especially when PUFA chain lipids are present (*47, 49*). Supporting this view of segregation into organizationally distinct domains rich in PUFA and in saturated fatty acid was previously seen in a mixed membrane composed of 1-palmitoyl-2-docosahexaenoylphosphatidyethanolamine (16:0−22:6PE, PDPE) and sphingomyelin (SM) (1:1 mol) (*49*). Differential scanning calorimetry (DSC) and solid-state ^{2}H NMR revealed the presence of disordered PDPE-rich and ordered SM-rich domains which were <20 nm in size. Cholesterol was preferentially found in SM-rich domains, serving to further exclude PDPE into the PDPE-rich domains.

Having said this, the pronounced differences between DMPC-doped and POPC-doped DAPC bilayers are not observed in MD simulations, although at 10 mol % dopant concentrations (i.e., DMPC or POPC) the simulations indicate that more cholesterol adopts the upright orientation in a DMPC-doped DAPC bilayer as compared to a POPC-doped DAPC bilayer (black curves in
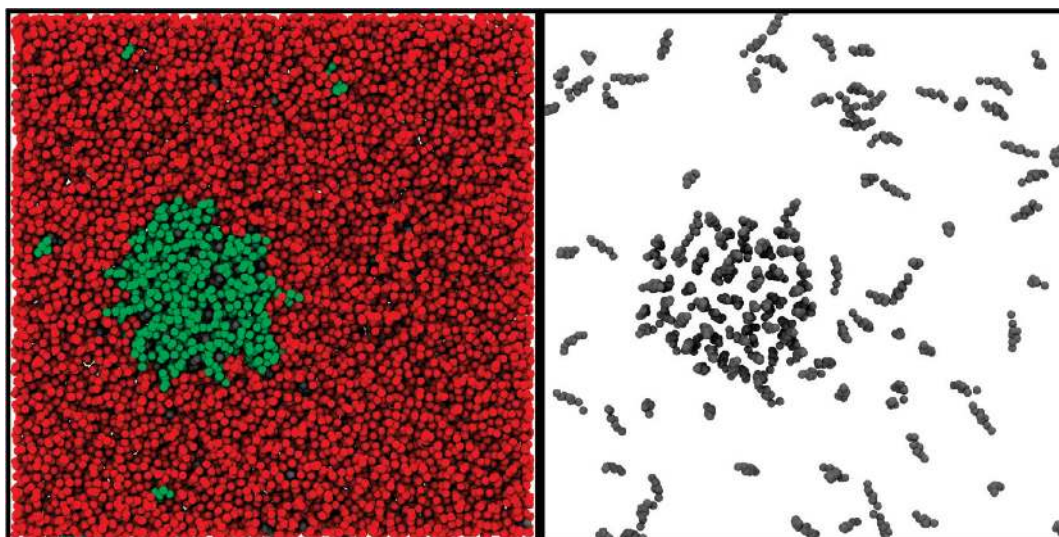
FIGURE 6: Snapshots (top view) of an MD simulation of a DAPC bilayer doped with 10 mol % DMPC and 10 mol % cholesterol (the simulation system is comprised of 1520 lipid and cholesterol molecules in total). DAPC molecules are shown in red, DMPC in green, and cholesterol in gray; water molecules are not shown for visual clarity. Left: A DMPC-rich domain (green) in a DAPC bilayer (red). Right: Cholesterol molecules only. It is evident that a considerable amount of cholesterol resides outside the DMPC-rich domain. Importantly, cholesterol molecules in the PUFA-rich domain are laying flat in the bilayer center, whereas those in the DMPC-rich domain adopt, almost exclusively, the upright orientation. In neither orientation is distinct clustering (i.e., dimers or trimers) of cholesterol molecules observed.

Figure 5). It should be noted that the nonbonded interactions between cholesterol and the individual beads in DMPC and POPC chains, respectively, are the same in the MARTINI model, suggesting that any differences in the interactions of cholesterol with the two lipid species are predominantly steric in origin. Such subtle differences in the packing are challenging to capture at the coarse-grain level. An alternative explanation for the observed differences between simulation and experiment could be attributed to the limited system size of the MD simulation. For example, in the 5 mol % DMPC-doped system, only 80 saturated lipids are present (40 per monolayer), yielding an lo domain of about 5 nm in diameter (Figure 5). Since this diameter is comparable to the width of the lo/ld interface region (*39*), such small domains have ill-defined core regions (i.e., no extended pure lo phase).

Although the MD simulations presented here may contain too few molecules (1520 lipid and cholesterol molecules in total) to observe macroscopic domain formation, the demixing of lipids is observed in all systems, consistent with previous simulations of ternary mixtures (*39, 50*). Cholesterol in the lo domain mainly adopts an upright orientation between saturated lipid hydrocarbon chains, while in the remaining ld phase cholesterol preferably adopts a flat orientation in the PUFA-rich bilayer center (Figure 6). However, due to the predominance of the ld phase, there are considerable amounts of cholesterol found in this phase. Therefore, instead of the much widely used term of cholesterol-rich domains, our results support the previously suggested terminology of saturated lipid-rich domains (*40*).

CONCLUSIONS

The present data unambiguously make the case for cholesterol preferring certain lipids over others. For the present study, the order of preference is DMPC, POPC, and DAPC. The experimental data are also in agreement with the "umbrella" interaction model (*51*) according to which a saturated or monounsaturated PC lipid can "shield" about two cholesterol molecules, enabling cholesterol to avoid any energetically unfavorable interactions

with water. Our results further suggest that the cross-molecular interaction preference between the various components of the POPC−DAPC−cholesterol system is as follows: POPC−DAPC (PUFA), cholesterol−POPC, and cholesterol−DAPC (PUFA). In the case of the cholesterol−DAPC interaction, the highly disordered PUFA hydrocarbon chains cause cholesterol to sequester to the bilayer's center.

The DMPC-doped DAPC bilayers with 10 mol % cholesterol present us with some interesting notions. While 50 mol % POPC is necessary to flip cholesterol in DAPC bilayers into its upright orientation, only 5 mol % DMPC is needed to achieve the same effect. This result clearly demonstrates cholesterol's affinity for saturated chains. Furthermore, our experimental data convincingly demonstrate cholesterol's aversion to the disordered PUFA chains. These conclusions are also corroborated by coarse-grain MD simulations. As was reported previously by Marrink et al. (*22*), MD simulations have again shown that, at any given time there exists a distribution of cholesterol orientations in bilayers with high PUFA content, something that we are still unable to resolve by experiment. More importantly, however, MD simulations predict the formation of DMPC-rich domains, where cholesterol is located preferentially in its upright orientation, and domains depleted of DMPC, where cholesterol is found mostly in the bilayer center. Similar observations were also made by neutron diffraction in 10 mol % DMPC-doped DAPC bilayers but not in any mol % of the POPC-doped DAPC bilayers. We interpret this result as DMPC molecules avoiding to interact with PUFA chains by forming domains, further evidence supporting the idea that domain formation is driven by the aversion that certain lipids have for each other (*49*).

Biological systems are made up by a great number of different lipids and sterols. Dipolyunsaturated lipids like DAPC represent an extreme in PUFA content. Their study, particularly in relation to saturated lipids and cholesterol, provides a reference point in elucidating the role played by lipid species in determining membrane architecture. The present work clearly demonstrates the importance of different lipid species and their possible roles in membrane domain formation. In addition, although essentially

absent from most membranes, dipolyunsaturated phospholipids are present in neural membranes where the influence that they exert on membrane organization is essential in controlling protein activity (*48, 52, 53*). Rhodopsin, the visual pigment in the retinal rod outer segment (ROS), is a prime example. The distribution of PUFA and cholesterol in the column of disk-like membranes that constitute the ROS is consistent with the results presented here. There, the amount of DHA (docosahexaenoic 22:6 acid) and sterol increases and decreases, respectively, from basal to apical ends of the rod (*54*).

REFERENCES

1. Singer, S. J., and Nicolson, G. L. (1972) The fluid mosaic model of the structure of cell membranes. *Science 175*, 720–731.
2. Dopico, A. M., and Tigyi, G. J. (2007) in Methods in Membrane Lipids, pp 1–13, Humana Press, Totowa, NJ.
3. Calder, P. C., and Yaqoob, P. (2007) Lipid rafts—composition, characterization, and controversies. *J. Nutr. 137*, 545–547.
4. Mitchell, D. C., and Litman, B. J. (1998) Effect of cholesterol on molecular order and dynamics in highly polyunsaturated phospholipid bilayers. *Biophys. J. 75*, 896–908.
5. Pitman, M. C., Suits, F., Mackerell, A. D., Jr., and Feller, S. E. (2004) Molecular-level organization of saturated and polyunsaturated fatty acids in a phosphatidylcholine bilayer containing cholesterol. *Biochemistry 43*, 15318–15328.
6. Silvius, J. R. (2003) Role of cholesterol in lipid raft formation: lessons from lipid model systems. *Biochim. Biophys. Acta 1610*, 174–183.
7. Smith, L. L. (1991) Another cholesterol hypothesis: cholesterol as antioxidant. *Free Radical Biol. Med. 11*, 47–61.
8. Petrie, R. J., Schnetkamp, P. P., Patel, K. D., Awasthi-Kalia, M., and Deans, J. P. (2000) Transient translocation of the B cell receptor and Src homology 2 domain-containing inositol phosphatase to lipid rafts: evidence toward a role in calcium regulation. *J. Immunol. 165*, 1220–1227.
9. Papanikolaou, A., Papafotika, A., Murphy, C., Papamarcaki, T., Tsolas, O., Drab, M., Kurzchalia, T. V., Kasper, M., and Christoforidis, S. (2005) Cholesterol-dependent lipid assemblies regulate the activity of the ecto-nucleotidase CD39. *J. Biol. Chem. 280*, 26406–26414.
10. Aittoniemi, J., Rog, T., Niemela, P., Pasenkiewicz-Gierula, M., Karttunen, M., and Vattulainen, I. (2006) Tilt: major factor in sterols' ordering capability in membranes. *J. Phys. Chem. B 110*, 25562–25564.
11. Khelashvili, G., Pabst, G., and Harries, D. (2010) Cholesterol orientation and tilt modulus in DMPC bilayers. *J. Phys. Chem. B 114*, 7524–7534.
12. Pan, J., Tristram-Nagle, S., and Nagle, J. F. (2009) Effect of cholesterol on structural and mechanical properties of membranes depends on lipid chain saturation. *Phys. Rev. E: Stat., Nonlinear, Soft Matter Phys. 80*, 021931.
13. Kučerka, N., Pencer, J., Nieh, M. P., and Katsaras, J. (2007) Influence of cholesterol on the bilayer properties of monounsaturated phosphatidylcholine unilamellar vesicles. *Eur. Phys. J. E 23*, 247–254.
14. Kučerka, N., Perlmutter, J. D., Pan, J., Tristram-Nagle, S., Katsaras, J., and Sachs, J. N. (2008) The effect of cholesterol on short- and long-chain monounsaturated lipid bilayers as determined by molecular dynamics simulations and X-ray scattering. *Biophys. J. 95*, 2792–2805.
15. Kučerka, N., Marquardt, D., Harroun, T. A., Nieh, M. P., Wassall, S. R., and Katsaras, J. (2009) The functional significance of lipid diversity: orientation of cholesterol in bilayers is determined by lipid species. *J. Am. Chem. Soc. 131*, 16358–16359.
16. Wassall, S. R., Brzustowicz, M. R., Shaikh, S. R., Cherezov, V., Caffrey, M., and Stillwell, W. (2004) Order from disorder, corralling cholesterol with chaotic lipids. The role of polyunsaturated lipids in membrane raft formation. *Chem. Phys. Lipids 132*, 79–88.
17. Lands, W. E. (1992) Biochemistry and physiology of n-3 fatty acids. *FASEB J. 6*, 2530–2536.
18. Stillwell, W., and Wassall, S. R. (2003) Docosahexaenoic acid: membrane properties of a unique fatty acid. *Chem. Phys. Lipids 126*, 1–27.
19. Simopoulos, A. P. (1999) Essential fatty acids in health and chronic disease. *Am. J. Clin. Nutr. 70*, 560S–569S.
20. Harroun, T. A., Katsaras, J., and Wassall, S. R. (2006) Cholesterol hydroxyl group is found to reside in the center of a polyunsaturated lipid membrane. *Biochemistry 45*, 1227–1233.
21. Harroun, T. A., Katsaras, J., and Wassall, S. R. (2008) Cholesterol is found to reside in the center of a polyunsaturated lipid membrane. *Biochemistry 47*, 7090–7096.
22. Marrink, S. J., de Vries, A. H., Harroun, T. A., Katsaras, J., and Wassall, S. R. (2008) Cholesterol shows preference for the interior of polyunsaturated lipid membranes. *J. Am. Chem. Soc. 130*, 10–11.
23. Vist, M. R., and Davis, J. H. (1990) Phase equilibria of cholesterol/dipalmitoylphosphatidylcholine mixtures: ^{2}H nuclear magnetic resonance and differential scanning calorimetry. *Biochemistry 29*, 451–464.
24. Léonard, A., Escrive, C., Laguerre, M., Pebay-Peyroula, E., Néri, W., Pott, T., Katsaras, J., and Dufourc, E. J. (2001) Location of cholesterol in DMPC membranes. A comparative study by neutron diffraction and molecular mechanics simulation. *Langmuir 17*, 2019–2030.
25. Marsan, M. P., Muller, I., Ramos, C., Rodriguez, F., Dufourc, E. J., Czaplicki, J., and Milon, A. (1999) Cholesterol orientation and dynamics in dimyristoylphosphatidylcholine bilayers: a solid state deuterium NMR analysis. *Biophys. J. 76*, 351–359.
26. Mathai, J. C., Tristram-Nagle, S., Nagle, J. F., and Zeidel, M. L. (2008) Structural determinants of water permeability through the lipid membrane. *J. Gen. Physiol. 131*, 69–76.
27. Katsaras, J., and Watson, M. J. (2000) Sample cell capable of 100% relative humidity suitable for x-ray diffraction of aligned lipid multibilayers. *Rev. Sci. Instrum. 71*, 1737–1739.
28. Als-Nielsen, J., and McMorrow, D. (2001) Elements of Modern X-Ray Physics, John Wiley & Sons, New York.
29. Kučerka, N., Nieh, M. P., Pencer, J., Sachs, J. N., and Katsaras, J. (2009) What determines the thickness of a biological membrane. *Gen. Physiol. Biophys. 28*, 117–125.
30. Wiener, M. C., King, G. I., and White, S. H. (1991) Structure of a fluid dioleoylphosphatidylcholine bilayer determined by joint refinement of x-ray and neutron diffraction data. I. Scaling of neutron data and the distributions of double bonds and water. *Biophys. J. 60*, 568–576.
31. Marrink, S. J., Risselada, H. J., Yefimov, S., Tieleman, D. P., and de Vries, A. H. (2007) The MARTINI force field: coarse grained model for biomolecular simulations. *J. Phys. Chem. B 111*, 7812–7824.
32. Hess, B., Kutzner, C., van der Spoel, D., and Lindahl, E. (2008) GROMACS 4: algorithms for highly efficient, load-balanced, and scalable molecular simulation. *J. Chem. Theory Comput. 4*, 435–447.
33. Gordeliy, V. I., and Chernov, N. I. (1997) Accuracy of determination of position and width of molecular groups in biological and lipid membranes via neutron diffraction. *Acta Crystallogr., Sect. D: Biol. Crystallogr. 53*, 377–384.
34. Kučerka, N., Nagle, J. F., Sachs, J. N., Feller, S. E., Pencer, J., Jackson, A., and Katsaras, J. (2008) Lipid bilayer structure determined by the simultaneous analysis of neutron and X-ray scattering data. *Biophys. J. 95*, 2356–2367.
35. Gennis, R. B. (1989) Biomembranes, Springer-Verlag, New York.
36. Knapp, H. R., Hullin, F., and Salem, N., Jr. (1994) Asymmetric incorporation of dietary n-3 fatty acids into membrane aminophospholipids of human erythrocytes. *J. Lipid Res. 35*, 1283–1291.
37. Brown, D. A., and London, E. (2000) Structure and function of sphingolipid- and cholesterol-rich membrane rafts. *J. Biol. Chem. 275*, 17221–17224.
38. Huang, J., Buboltz, J. T., and Feigenson, G. W. (1999) Maximum solubility of cholesterol in phosphatidylcholine and phosphatidylethanolamine bilayers. *Biochim. Biophys. Acta 1417*, 89–100.
39. Risselada, H. J., and Marrink, S. J. (2008) The molecular face of lipid rafts in model membranes. *Proc. Natl. Acad. Sci. U.S.A. 105*, 17367–17372.
40. Karmakar, S., Sarangi, B. R., and Raghunathan, V. A. (2006) Phase behaviour of lipid-cholesterol membranes. *Solid State Commun. 139*, 630–634.
41. Smith, G. S., Safinya, C. R., Roux, D., and Clark, N. A. (1987) X-ray study of freely suspended films of a multilamellar lipid system. *Mol. Cryst. Liq. Cryst. 144*, 235–255.
42. Chu, N., Kučerka, N., Liu, Y., Tristram-Nagle, S., and Nagle, J. F. (2005) Anomalous swelling of lipid bilayer stacks is caused by softening of the bending modulus. *Phys. Rev. E: Stat., Nonlinear, Soft Matter Phys. 71*, 041904.
43. Bennett, W. F., MacCallum, J. L., Hinner, M. J., Marrink, S. J., and Tieleman, D. P. (2009) Molecular view of cholesterol flip-flop and chemical potential in different membrane environments. *J. Am. Chem. Soc. 131*, 12714–12720.
44. Leventis, R., and Silvius, J. R. (2001) Use of cyclodextrins to monitor transbilayer movement and differential lipid affinities of cholesterol. *Biophys. J. 81*, 2257–2267.
45. Zhang, Z., Lu, L., and Berkowitz, M. L. (2008) Energetics of cholesterol transfer between lipid bilayers. *J. Phys. Chem. B 112*, 3807–3811.
46. Shaikh, S. R., Cherezov, V., Caffrey, M., Soni, S. P., LoCascio, D., Stillwell, W., and Wassall, S. R. (2006) Molecular organization of

cholesterol in unsaturated phosphatidylethanolamines: X-ray diffraction and solid state ^{2}H NMR reveal differences with phosphatidylcholines. *J. Am. Chem. Soc. 128*, 5375–5383.

47. Niu, S. L., and Litman, B. J. (2002) Determination of membrane cholesterol partition coefficient using a lipid vesicle-cyclodextrin binary system: effect of phospholipid acyl chain unsaturation and headgroup composition. *Biophys. J. 83*, 3408–3415.

48. Polozova, A., and Litman, B. J. (2000) Cholesterol dependent recruitment of di22:6-PC by a G protein-coupled receptor into lateral domains. *Biophys. J. 79*, 2632–2643.

49. Soni, S. P., LoCascio, D. S., Liu, Y., Williams, J. A., Bittman, R., Stillwell, W., and Wassall, S. R. (2008) Docosahexaenoic acid enhances segregation of lipids between raft and nonraft domains: ^{2}H-NMR study. *Biophys. J. 95*, 203–214.

50. Apajalahti, T., Niemela, P., Govindan, P. N., Miettinen, M. S., Salonen, E., Marrink, S. J., and Vattulainen, I. (2010) Concerted diffusion of lipids in raft-like membranes. *Faraday Discuss. 144*, 411–430.

51. Huang, J., and Feigenson, G. W. (1999) A microscopic interaction model of maximum solubility of cholesterol in lipid bilayers. *Biophys. J. 76*, 2142–2157.

52. Aveldano, M. I. (1989) Dipolyunsaturated species of retina phospholipids and their fatty acids. *Colloq. INSERM 195*, 87–96.

53. Brown, M. F. (1994) Modulation of rhodopsin function by properties of the membrane bilayer. *Chem. Phys. Lipids 73*, 159–180.

54. Albert, A. D., Young, J. E., and Paw, Z. (1998) Phospholipid fatty acyl spatial distribution in bovine rod outer segment disk membranes. *Biochim. Biophys. Acta 1368*, 52–60.